Journal of Materials and Applications 2021;10(2):90-99
https://doi.org/10.32732/jma.2021.10.2.90

Suitable Na_2O-SiO_2, BaO-SiO_2 Based Coatings for Stainless Steels

A. Faeghinia*, E. Jabbari

Ceramic Division, Materials and Energy Research Center, P.O. Box 14155-4777, Tehran, Iran
E-mail: a.faeghinia@merc.ac.ir (Corresponding author)

Received: 4 July 2021; Accepted: 6 September 2021; Available online: 25 October 2021

Abstract: Two frites with 40 wt.%SiO_2-20 wt.%B_2O_3-17 wt.%Na_2O (G1) and 42wt.%SiO_2-24wt.%BaO-18 wt.%CoO (G2) compositions were prepared and applied on stainless steel by the slurry method. The samples were heated at 950ºC (G2) and 860ºC (G1). The XRD results revealed the sodium silicate and barium silicate phases as well as almost 770 HV, 543 HV microhardness in G1 and G2 coats respectively. The thermal expansion coefficients were $\alpha=10.9\times10^{-6}$/K(G1) and $\alpha=13.31\times10^{-6}$/K (G2) respectively. According to EDS results the alkaline earth ions (and CoO) migration into the glass- steel interface was occurred in both coats. The dry sliding friction and wear behavior were investigated using a 4mm diameter AISI52100 steel pin on disk geometry under 5,10 and 18 N loads. The average wear rate were w.r: 32×10^{-14}(m^3/N.m) and w.r:5×10^{-14}(m^3/N.m) in G1 and G2 coats. Then two frites were mixed and heat treated at 800ºC with high heating and cooling rate. The resulted composite (G1-G2) shows almost the average wear rate 4×10^{-14}(m^3/N.m), while the coefficient friction of G1-G2 composite was not improved significantly.
Keywords: Aluminosilicate glass; Coating; Wear; Cobalt/cobalt compounds; Glass-ceramic.

1. Introduction

The barium silicate (BS) glass and glass –ceramic materials are well known as a suitable candidate for sealing in planar SOFCs. They have good thermal expansion compatibility and long term stability with the metal substrate and have desire adhesion to the steel substrate [1]. The main point of this enamels is that the steel substrate should be pre-oxidized, prior to the enameling to adhesion to this glaze. Otherwise, if the peroxidation procedure omitted (the oxide phase of the steel surface was avoided) the BS enamels for better adhesion should be reinforced with the reducible metal oxide like CoO_3 and or MoO_3 [2]

Recently the cobalt containing BS glass-ceramic has evaluated as shock resistance material for use in boiler tubes of power plants [3]. They performed the thermal shock test at 600 – 900 º C in muffle furnace, and showed that the CoO containing glass – ceramic coating endured more than 50 times of thermal cycling. In addition, they displayed that, steel loss reduced to nearly zero. Thus they suggested that this behavior could greatly expands the usage of stainless steel in a variety of temperature range [4]. The tribological and wear behavior of BS glass-ceramic were not studied yet. On the other hand, in concrete industry, it was reported that the sodium silicate on steel surface produced strong bond with concrete, which increases the wear resistance of concrete [5]. Therefore, it can be said that sodium silicate formation helps the bonding of studied glass and the steel substrate. In this system the peroxidation of steel is required as well.

Sodium alumina silicate based glass–ceramic coating for gas turbine engine components has been reported recently. The oxidation resistance and the COF of this material was evaluated [6]. However, the detail of sintering, crystallization and microstructure, thermal expansion and the wear rate of this composition were not studied before.

The idea of mixing two frites were reached to avoid the peroxidation step in coating procedure. Also,

we supposed that since the mixed frites of two BS and Sodium alumina silicate have both thermal shock and oxidation resistance, so the sintering conditions of the mixed frites will not need the controlled cooling in sintering procedure.

In this study the thermo- physical, sintering condition and wear properties of mentioned BS and Sodium alumina silicate coats were first studied individually and the resulted wear rate and COF mixed composite were evaluated.

On the other hand we considered the Co price in glaze recipe could be decreased by Sodium alumina silicate glass-ceramic as filler.

2. Experimental procedure

Two frits were prepared from reagent grade chemicals: SiO_2 (industrial azandarian silica, 99.9% purity), Al_2O_3(KMS-96 MARTOXID), $BaCO_3.10H_2O$,(Industrial grade, alborz company, Esfahan) $CaCO_3$,(Industrial grade, birjand area), Na_2CO_3(Merck, CAS No. 497-19-8, EC), ZnO (Merck, CAS No. 1314-13-2), $H_2P_2O_5$, CoO and CaF_2. The chemical compositions of the frits G1 and G2 are listed in Table 1.

Table1. The chemical composition of the G 1 and G2

	SiO_2	Al_2O_3	ZnO	BaO	B_2O_3	CaO	CoO	MoO_3	P_2O_5	Na2O
G1	42	3	4	24	3.5	4	18	1.5	-	-
G2	40	11	8	-	20	2	-	-	2	17

The batches were melted in an alumina crucible in a resistance furnace at 1250˚C-1350˚ C temperatures, for 2 h. Then the batches were quenched into the water to produce the frits .The frits were milled using a ball mill with alumina balls as the grinding media for 24 h. and screened with 200 mesh size, stored in an oven at 100˚C to remove the moisture. The powder size distributions determined by laser diffraction using a Malvern Master Sizer 2000. Are shown in Figs. 1a and b.

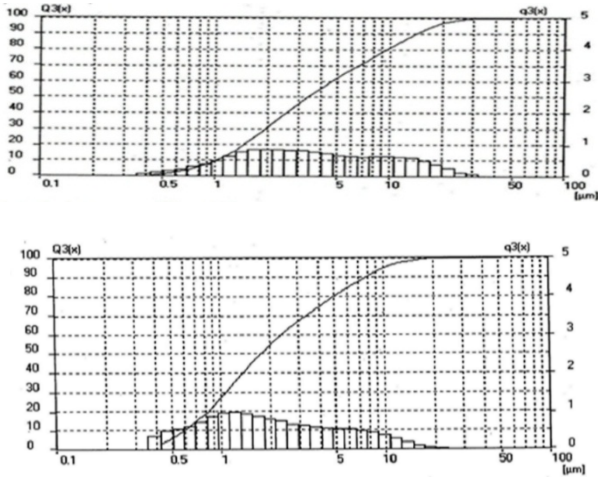

Fig.1 The particle size distribution of(a) G2 frits (b) G1 frit

The powder typically exhibits a Gaussian distribution in particle size with a cumulative weight percent average of ≈5 µm. The fine powder particles exhibit an X-ray diffraction pattern typical of an amorphous structure with a broad amorphous hump and lack of Bragg diffraction peaks (Fig. 2).

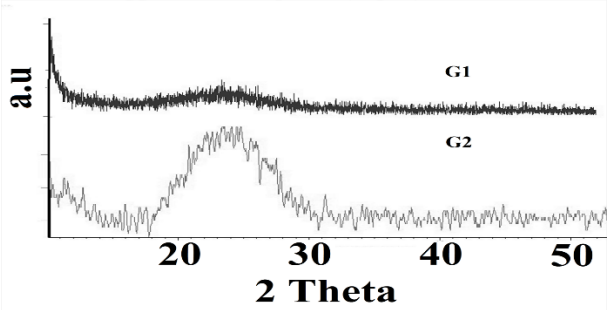

Fig.2 The XRD pattern of G1 and G2 frits

The frits were further processed by mixing with certain mill-additive (Kaolinite,The *Kaolin*, supplied from Zonoz mines, *Marand*, Iran)., borax and water, Sb_2O_3, MoO_3) to make thick slurry called "slip" and to make uniform and thin coating on the clean metal parts(without peroxidation) by spraying technique .(Table 2).

Table 2. The chemical compositions of two obtained slurry from G1and G2

	Frit	Clay	Borax	Water	Sb_2O_3	MoO_3
Slurry of G1	100	7	1	50		
Slurry of G2	100	3	-	60	1.3	2.9

The mass ratio of solid to water in all mixtures was 78/ 22. Aqueous frit suspensions at 70 vol. % solid loading were prepared by using Sodium Alginate (1.2 wt. % based on solid weight) as dispersant. The rheological properties of coating material slips are very important in point view of proper application of the coating. The specific gravity of the enameling slip was controlled between (1.7-1.8 g/cm^3) by adjusting the water content. Subsequently, the slip was aged for 24 hours before enameling to improve its fluidity. The G1-G2 enamel was also prepared by mixing the two different G1 and G2 frites with 50-50 weight ratio and then the resulted composite was sintered at 800ºC with 15 minutes holding time and with the 20ºC/min heating rate and fast cooling. These conditions were obtained to reach the glossy adequate enamel's appearance.

Steels samples (316 alloy) were obtained by cutting annealed 1.5 in. diameter. The bars stock into disks of 5 mm thickness, which were then cut into quarter-disk coupons for testing. The steel substrates were blasted to give a surface with a R_a value of 2 mm. immediately before spraying. The Air Spray coatings were manufactured using nozzle with 0.5 mm. internal diameter, using an argon. Slips were injected externally of the nozzle using an inject or of 0.5 mm. in internal diameter, Particles were carried into the jet by argon gas having a flow rate of 7 SLM and setting the powder flow rate in 30 g/ min. The standoff

distance was 100 mm. The green deposit was slowly dried in air, followed by heating in an air oven at ~120 °C for complete drying. The weight of the deposit (0.2 g) was measured by weighing the plates before and after the deposition Subsequently, the coatings were examined visually for surface quality.

Crystallization of products (glass-ceramics) in powder form were identified by XRD (Philips power diffractometer 1710). Cu Kα radiation was used in XRD examinations. Working voltage and current were 40 kV and 80mA, respectively, and the step size and step time were 0.04◦ and 0.75 s respectively. The hardness of the specimens was measured with a Vickers micro-hardometer model (HVS-1000). The hardness tests were performed under an indentation load of 20 g for 20 s. Scanning electron microscopy (SEM: model JEOL JXA-840) was used in order to observe the microstructure and EDS analysis. Samples were mounted onto the sample holder, coated with gold and then studied with SEM.

Pin-on-disk the most widely used wear test processes, followed by pin-on-flat. Other applications of pin-on-disc include material wear and friction properties at elevated temperatures and in controlled atmospheres .

Wear tests were performed in accord with the ASTM:G99-95a for wear testing with a pin-disk. The counter specimen was a pin mad from ball bring steel 52100 (micro hardness 66 Rockwell C). a load at frictional contact was F = 18 N, linear sliding speed was v = 0.5 m/s, total sliding length was s = 200 m, friction radius was rt = 13 mm. The wear rate expressed in (mg/m) is calculated as follows:

$$W_R = \frac{\Delta w}{S.F}$$

Where: wear rate, Δw: weight loss in (mg), s sliding distance in (m). A wear coefficient is often used to categories resistance to contact wear. (All of the tests were conducted at ambient atmospheric condition at room temperature (25) ˚C and 23% humidity. Lubrication is not applied to avoid the complication of thermochemical effects.

3. Results and discussion

Fig.3 represents the DTA results of G1 and G2 frites. The curve related to the G1 glass, indicated to T_g (620°C glass transition temperature) and sharp T_p (639°C bulk crystallization temperatures), respectively. The endothermic peak at 870ºC pointed to the melting of at least one of the crystalline phases, formed at low temperature. In the case of G2, the single broad exothermic effect at 721°C assigned probably to the surface crystallization and the other peak (976°C) correspond to the melting of remainder phase. It is clear that the G2 glass has the higher thermal stability and refractoriness compared to G1 and has higher melting temperature, which can be led to the rigid structure of this glass [7]. It can be seen that the T_g peak in G2 sample is not very sharp which could be related to the high viscosity or phase separating of this glass compared to the G1 one. The higher amount of alkaline earth oxide BaO+CaO (28 wt.%) in G1 glass could decrease the characteristic temperatures while the G2 glass has only 17% Na_2O [3].

The G1 coating, was heat treated at three steps first at 870 ºC (5min), which followed by heating at 620ºC (30min) and 639ºC (30min) respectively. The first heating was done to get a dense, continues semi melted glass cover over the steel surface and the second heat-treatment was performed to reach the crystallization. This procedure is different from other's heating reports [3, 6]. G2 coating was heat-treated at 950ºC - 5min. 620ºC - 30min, 720ºC -30min. continuously. The heating and cooling rates in all cases were approximately 10ºC/min. sharp XRD pattern of Barium calcium silicate was detected which formed in G2 glass-ceramic. It means that by frit grinding the crystallization of this glass was enhanced [1]. Typical XRD patterns of obtained glass-ceramic samples were presented in Fig. 4.

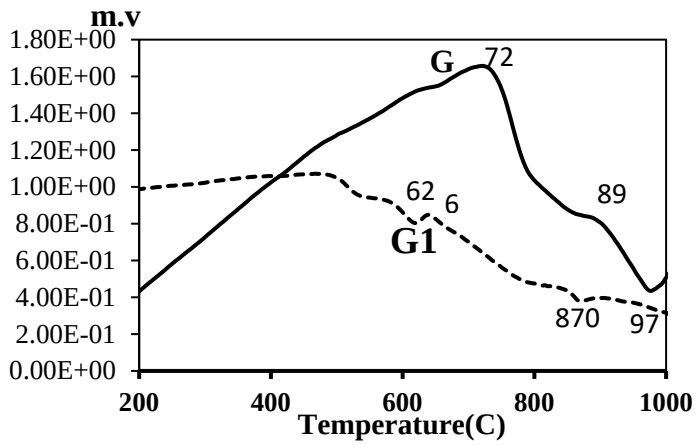

Fig. 3. The DTA results of G1, G2 frits, The characteristic peaks are detected at (G1:620ºC,639ºC,), (G2:640ºC,721ºC)

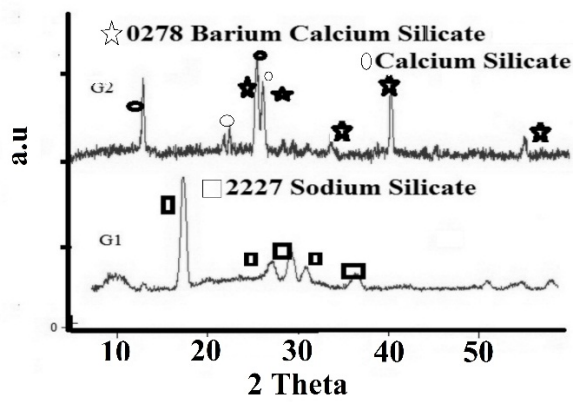

Fig.4. The XRD patterns of heat-treated G1 and G2

The sodium silicate phase with almost weak XRD peaks intensity was detected, it was the major crystalline phase in G1 glass-ceramic. It can be seen that although the G1 enamel has Ca^{+} element in its composition, but the Ca^{2+} ion was not entered into the sodium silicate glass-ceramic system.

3.1 Dilatometer results

Fig. 5 shows the thermal expansion coefficients (TEC) of the two G1 and G2 glasses. As it can be seen the thermal expansion coefficient of the G1 glass is approximately $\alpha=10.99\times10^{-6}$ /K while the G2 glass has $\alpha=13.31\times10^{-6}$ /K these properties indicated that open structure of G2 glasses can led to the higher TEC values [8]. The thermal stability of G2 glass was proved in DTA results as well. It is well known that the BaO in seal glasses were used to decrease the TEC values [2].

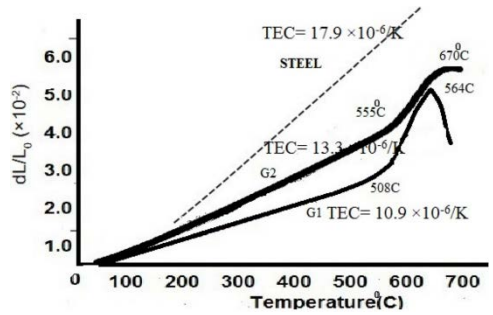

Fig.5. The thermal expansion coefficient (TEC) of G1 and G2 glasses

The different TEC values of the coatings and substrate will caused to the thermal expansion mismatch with the steel substrate and will caused the different compressive stress on the surface of resulted enamels [9]. A general

trend in all metal systems is to use coating with slightly lower thermal expansion coefficients compared with that of the substrate resulting in a positive mismatch in thermal expansion coefficient (+Δ TEC). The concept behind this TEC mismatch is to generate compressive stresses in the weaker glaze and thus enhance the overall strength of the coating. This technique had excellent results with porcelain fused to metal restorations (PFM) [10]. However, there are concerns to apply this concept to all-ceramic coatings.

Also it is obvious from the dilatometer results that, the G2 glass composition perhaps has phase separation that needs the long annealing time for achieving the dense structure while the G1 glaze shows the deep expansion alteration with temperature, that points to the good anneal ability of this composition [11].

3.2 Microstructural evaluation of interface

In order to evaluate the exact trace elements of the enamel's surface and the interface with the steel, the EDS analysis was done on enamel, to detect the elements migration after sintering, to estimate the surface composition and finally the resulted glass's properties of enamels.

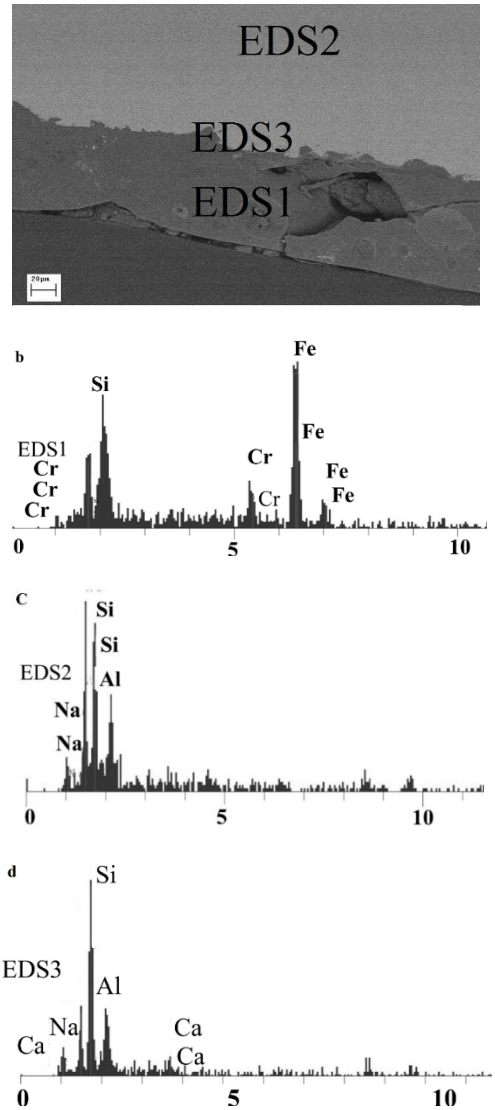

Fig.6. (a) SEM micrograph of G1 enamel and interface, EDS results of (b) the enamel side of G1 denoted by EDS2 (c) the interface layer by EDS3 and (d)the steel substrate side denoted by EDS1

The microstructure of G1 was presented in Fig. 6a. The cross-sectional microstructures and the data from EDS examination of the polished cross-section of the glass-ceramic coating are presented in Fig. 6b. In the case of G1, probably, the galvanic corrosion of the base iron by glassy silicate phase at selective random points, caused to the increased roughness of interface [12]. This roughness could improve the mechanical coupling (Fig.6a). It was reported that the more alkaline in the silicate glass composition (EDS2) helps the adhesion of silicate to steel substrate (Fig.6b) [13]. Beside the silicate, the alkaline oxide assists the Fe recharching at the silicate –iron oxide

interface [14], while the alkaline earth oxide (Like Ca^{2+}ions) acts vice versa and may has migrated to the iron oxide –silicate interface (EDS3) (Fig.6c). The EDS2 result in Fig. 6b proved the migration of listed above oxides (CaO and SiO_2) to the boundary layer .(see also the EDS1 result in Fig. 6d). It can be said that the Al and Na ions have already been remained in the glassy phase of enamel, while the Ca^{2+} ions were transferred to the boundary layer. However, the Ca^{2+} ions were trace in the boundary (G1 glass composition) and the enamel has coated on the steel substrate.

3.3 G2 evaluation

It was shown that, [14] in the case of alkaline earth metal oxide (like considerable amount of BaO in G2 composition), these ions decreased the recharging effect of the silicates and give the weak adherence of enamel to substrate. So, the CoO composition has been used as adherence agent in this composition. The good adhesion of G2 (CoO bearing frit) to stainless steel substrate can be seen in Fig.7.

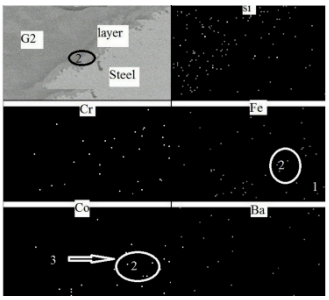

Fig.7. The elemental map analysis of G2 and steel. The areas denoted by 2 and 3 relate to the interface and G2 enamel side, respectively

It can be seen that the boundary layer between enamel and substrate was formed. The interface contains Cobalt oxide on the substrate side, while it was decreased on the coating surface side. It is well known that Cobalt oxide of the enamel will reduced to cobalt metal and will form a bond with the iron and the enamel. Oxygen in the muffle penetrates the enamel during the early stages of the firing forming a film of iron oxide on the surface of the steel [15]. This film, whether applied before enameling or formed incidentally to firing, partially dissolves in the fused enamel giving the intimate bond between metal and enamel.

According to map (Fig.7) the outward diffusion of Fe ions from the stainless steel and Co^{2+} ions from the glass was happened. It is certain that a Co-Fe rich layer exists in the bonding section of the coated sample.

$$Fe\ (substrate) + Co^{2+}(II) = Fe^{2+(I)} + Co$$

From the map results a trend can be seen where there is an increase of iron content from 1 to 2 and an increase of the Co concentrate from 3 to 2 (areas). These results show a proof of diffusion mechanism of iron from substrate to interface layer and the diffusion mechanism of Co^{2+} from enamel to interface. The Ba^{2+} ions migration also was recorded in this map and it was shown that the Barium ions almost have spread adequately and no evidence of this ion migration was seen.

As the sintering temperature increases, the migrated ions with higher covalent, Ca in G1 and Co in G2 Adhered to the substrate surface, these ions lead the interlayer glass's Ts to be decreased [9]. Consequently, the ratio of T_s /T_m (T_m is the melting point of the surface of the coating material) becomes lower. This caused to a decrease in the degree of mismatch between the coating and the substrate [9]. The combination of these factors makes compressive residual stress greater.

3.4 Micro hardness evaluation

The microhardness of enamels on the different substrate were evaluated. Table 3 shows the obtained results of the microhardness of glass-ceramic coatings .It should be borne in the mind that the presence of thermally originated residual compressive stress on the surface might cause an apparent increase in the hardness value [16, 17] .

Table 3. The average microhardness of resulted G1and G2 enamels

sample	G1	G2
microhardness	777.4HV	543HV

These values (777 HV of sodium silicate glass-ceramic) are considerably higher than the other LAS reported glazes [18]. In the case of sodium silicate glass –ceramic, it was reported [19] that if the clay size, used in the enamel slurry, decreased to nano size, the hardness of sodium silicate base glass ceramic will be up to 700HV, which the present enamel has almost the same hardness without using nano size clay. In addition, the worked barium silicate glass-ceramic comparing to dental barium silicate composites [10] shows lower hardness which could be related to the Cobalt oxide content of this glass-ceramic, that has not been used in dental composites. Also it can be said that the G1 sample has more compacted glass structure compared to the G2 glass which could increase the residual glass of this system.

3.5 Wear behavior

The weight loss vs. sliding distance of the two individual G1 and G2 coatings under different applied loads (5, 10N) were shown in Fig. 8. The weight losses of samples vs. sliding distance, defines the wear rate and friction coefficient. According to results, while the G2 shows 4-mg. weight loss, in 150 m., the maximum weight loss of G1 is 2 mg in 100m. In comparison, a drastic reduction in wear loss is observed by using G1 composition which can be as reinforcements for making hybrid composite with G2 composition. In addition, the weight loss of the 50 wt. .% G1-50 wt.% G2 compositions by applying the 10 N load was presented in Fig.8.

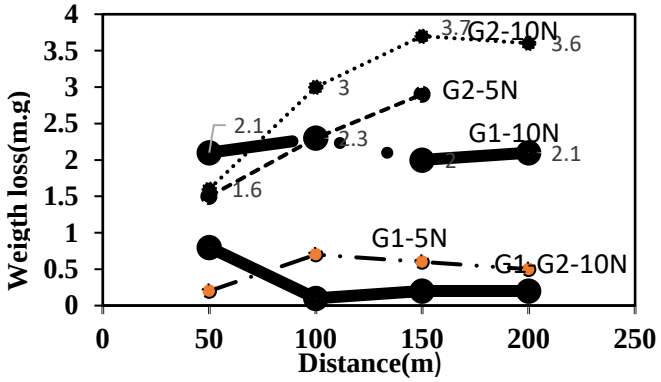

Fig.8. The weight loss of samples versus distance at different loads

Also, the wear rate of G1 and G2 and the composites of them by applying the 18N load were presented in Fig.9. Obviously, the wear rate of G2 glass ceramic is higher than the G1 glass-ceramic. It can be related to the low hardness value of G2 system. Also, considering the lower thermal expansion coefficient of G1 compared to G2, it can be said that the higher thermal mismatch of G1 glaze caused to more compressive stress. In some cases these stress are beneficial for the mechanical and tribological behavior of the component. For example, it has been shown that compressive stress in physical vapor deposited (PVD) coatings can increase their fracture strength. This effect is important since fracture and wear are normally initiated from flaws at the coating surface. Due to the relatively high sintering temperatures and the mismatch in coefficient of thermal expansion between coating and substrate, high residual strains are formed in the G1 coating upon cooling [20].

In addition, according to Fig. 9 the slop of wear rate vs. sliding distance for the initiation of mild wear was increased in the G1-G2 composite compared to G2 and G1 individually. This slop is a quantitative measure of the running- in behavior of the G2-G1 enamels and apparently depends on the applied load [21].

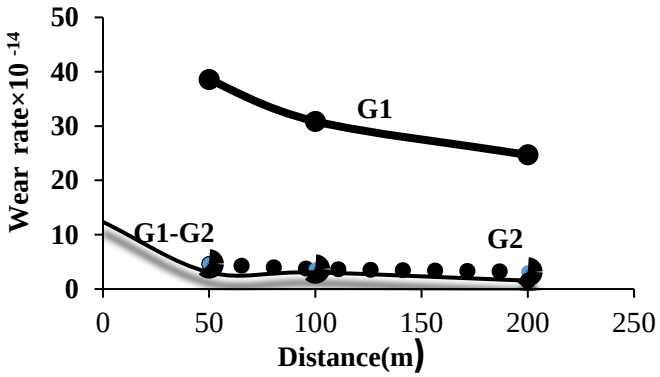

Fig.9. Wear rate of samples versus distance at 18N load and 0.02 m /s velocity, with 14 mm diameter

In addition, it can be said that by adding 50 wt. % of G1 composition to G2 enamel, the lowest wear rate in the steady state (at 10N loads) was achieved. It could be related to the G2 glass compressive stress, porosity and G1-G2 glass, which has been affected by G2 addition [22].

By comparing the results of Fig.8 and Fig.9, the differences were exhibited in the weight loss of enamels. Apparently by applying 10 N pressure the G1-G2 composite shows the 100 m sliding distance required for equilibrium mild wear with the minimum weight loss (compared to G1and G2) while by increasing the applied load to 18N, the wear rate of G1-G2 composite is comparable to the G1 one. It means by increasing the applied load, rapid increase of enamel wear occurs, may be resulted from the accumulation of glass-ceramics debris at the wear track [23].

The COF values of G2, G1, G1-G2 by applying 18N load were presented in Figs. 10(a),10(b),10(c) respectively. As shown, the initial COF value increased gradually to almost steady state, i.e. 1.5 (Fig.10 a), 1.3 (Fig.10b), 1.5 (Fig.10 c) in G2, G1, and G1-G2 respectively .The G1 enamel showed the long transition distance, indicating good performance in friction (Fig.10 b) [24].

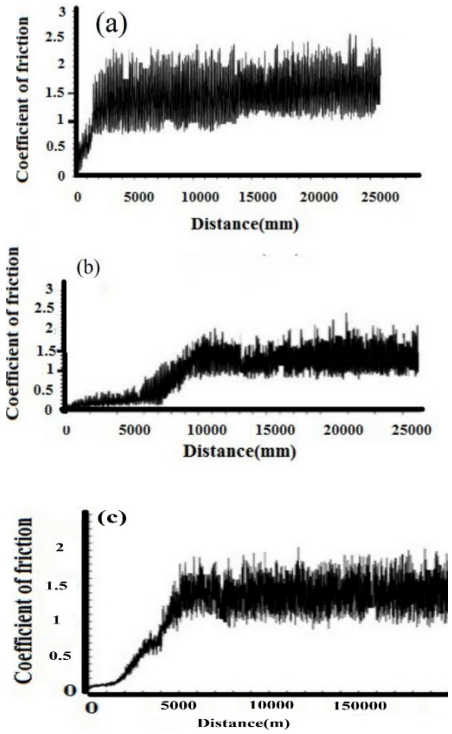

Figs. 10. The COF values of (a) G2 (b) G1 (c) G2-G1 enamels coated on steel substrate by applying 18 N load

This phenomenon can be related to the deposited glass-ceramic particles subjected to the almost high-18 N applied load [25], which is in agreement with other reports [20]. However, probably, the compressive stress extent on the surface of coats has not effect on COF values significantly (G2 and G1) moreover in the case of G1-G2 composite (Fig.10c) perhaps due to the two different roughness the resulted composite did not show the improved COF value (unlike the wear rate) [26].

4. Conclusion

Two glass compositions and the mixed of them by 40 wt.% SiO_2-20 wt.% B_2O_3-17 wt.% Na_2O (G1) and 42 wt.% SiO_2-24 wt.% BaO-18 wt.% CoO (G2) were prepared. They are suitable for application on steel alloys .The coatings were successfully applied as a single coat by simple vitreous enameling process onto already prepared (sand blasted) steel surfaces .The proposed coating material possesses a reasonable low melting (1250 ˚C-1350) and processing 620˚C-950 ˚C temperature, leading to the less cost and energy consumption during preparation and application .Sintering and crystallization of the two different silicate enamel groups and mixes of them were investigated. It was shown that the mixed coat was sintered at 800ºC which is considerably lower than the sintering temperature of the individual enamels.

Sodium silicate and barium calcium silicate were two phases of G1 and G2 glazes. It was shown that, the steel-glass interface changes considerably if Co is present (G2), Co-Fe layer alloy will formed on the glass-steel

interface. According to EDS analysis of G1 numerous silicate and calcium particles are dissipated in the case of sodium silicate enamel. This phenomena pointed to the alkaline silicate corresponded to the effectively in the discharging of the iron oxide surfaces [12]. The developed coatings exhibit high hardness values 573 HV in G1 to 777 HV in G2. The compressive stress resulted from thermal expansion mismatch between coats and steel substrate caused to the different wear rate. The low wear loss of G1 composition could mark it as reinforce for hybrid composite like G2-G1 composition. In addition, it can be said that by adding G1 composition to the G2 enamel, the lowest wear rate in the steady state was achieved. It could be related to the compressive stress, porosity, which has been affected by G1 addition [22]. In addition, the wear rate of 4×10^{-14}(m^3/N.m) for the 50 wt. .% G1-50 wt.% G2 compositions, by applying the 10 N loads, was recorded. But it has not effect on COF values significantly perhaps in G1-G2 composite due to different roughness the resulted composite did not show the improved COF value [26].

5. Acknowledgements

The author acknowledges the financial support of coating Project, Contract No. 93021874, from The Iran National Science Foundation (INSF).

6. References

[1] Namwong P, Laorodphan N, Thiemsorn W, Jaimasith M, Wannakon A and Chairuangsri T. A Barium-Calcium Silicate Glass for Use as Seals in Planar SOFCs. Chiang Mai Journal of Science. 2010; 37(2): 231-242.
[2] Burgel R, Kvenes I. Thermal Barrier Coatings. Proc. Conf. on High Temperature Alloys for Gas Turbines and Other Application. 1986, W. Betz et al.(eds). D. Reidel,Dordrecht, Publiching, 1986. p.327-356.
[3] Tanga W.X. Influence of CoO glass –ceramic coating on the anti-oxidation behavior and thermal shock resistance of 200 stainless steel at elevated temperature. Ceramic International. 2014; 40 (8):12327–12335.
[4] Majumdar A, Jana S. Glass and glass-ceramic coatings, versatile materials for industrial and engineering applications. Bulletin of Materials Science. 2001; 24(1): 69-7.
[5] Majumdar B.S and Newaz G.M. Constituent damage mechanisms in metal matrix composites under fatigue loading, and their effects on fatigue life. Materials Science and Engineering. 1995; A 200: 114-129.
[6] Datta S. Das S. A new high temperature resistant glass-ceramic coating for gas turbine engine components, Ceramics and Glasses. Bulletin of Materials Science. 2005; 28(7): 689-696.
[7] Majumdar A. Ganguli. D. Relative Reactivity's of Precursors in the Synthesis of Forsterite, Mg_2SiO_4. Transaction of Indian Ceramic Society.1995; 54 (6) :227-229.
[8] Cimek J, Liaros N, Couris S, Mariusz Klimczak R and Buczynski R. Experimental investigation of the nonlinear refractive index of various soft glasses dedicated for development of nonlinear photonic crystal fibers. Optical materials Express. 2017; 7 (10): 3471-3478.
[9] Bai Y, Gao K, Pang X, Yang H, Yan L, Volinsky A.A. Residual stress and microstructure effects on mechanical, tribological and electrical properties of TiN coatings on 304 stainless steel. Ceramics International. 2018; 44: 15851–15858.
[10] Borom M, Longwell A, Pask J. A. Reactions Between Metallic Iron and Cobalt Oxide-Bearing Sodium Disilicate Glass. Journal of the American Ceramic Society. 2006; 50(2):61 – 66.
[11] Kaura A, Khanna A, Marina H, Barriusob G, Gonzàlezb F. Effects of annealing on density, glass transition temperature and structure of tellurite, silicate and borate glasses. Journal of Non-Crystalline Solids. 2018; 500(15) : 443-452.
[12] Dingwell D.B. The solubility and oxidation state of nickel in silicate melt at low oxygen fugacities. Geochimica et Cosmochimica Acta. 1994; 58(8): 1967-1974.
[13] Yang X. Interactions between Iron Oxides and Silicates. Licentiate thesis Luleå University of Technology Department of Chemical Engineering and Geosciences Division of Chemistry SE-97187, Luleå, Sweden.
[14] Thi D. Ta, Bach H, Kiet T, Tribochemistry and Lubrication of Alkaline Glass Lubricants in Hot Steel Manufacturing. Lubricants. 2020; 8(7): 70-74.
[15] Yang X, Jha A, Brydson R, CochraneR.C. The effects of a nickel oxide pre coat on the gas bubble structures and fish-scaling resistance in vitreous enamels. Material Science and Engineering. 2004; A366: 254–261.
[16] Carriedo, M León, Gutiérrez CA, López-Cuevas J. The effect of residual stress on mechanical resistance of ZrSiO4/Al2O3 laminates. Boletín de la Sociedad. 2016;55(3):87-94.
[17] Lopez-Esteban S. et al. Spreading of Viscous Liquids at High Temperature: Silicate Glasses on Molybdenum. Langmuir. 2005; 21: 2438-2446.
[18] Al-Hasso F. Glass Coatings By Combustion Flame Spraying: the Microstructure and Properties. Universal Journal of Materials Science.2013; 1: 149-158.

[19] Podjuklová J, Suchankova K, Lanik T. An Effect of Clay Particles Size on Functional Features of Vitreous Enamel. Recent trends in structural materials. (2012), Plzeň, Czech Republic, EU.
[20] Ratia V, Heino V, Valtonen K, Vippola M, Kemppainen A, Siitonen P. Effect of abrasive properties on the high-stress three-body abrasion of steels. TRIBOLOGIA - Finnish Journal of Tribology. 2014; 1 (32):1-4.
[21] HanY, Pan F, Tang J, Zhou Ch. A Novel Wear Resistant Glass-Ceramic Coating Material. Materials Science Forum.2011; 686: 521-.527.
[22] Faeghinia A. Thermal properties and crystallization of lithium–mica glass and glass-ceramics. Thermochimica Acta.2013; 564: 1– 6.
[23] Faeghinia A, Zamanian A.Wear behavior of BCS glass ceramic coating on stainless still slab. Ceramics International. 2019; 45(1): 108-114.
[24] Maria G, Roberta C. In vitro wear of resin-based materials—Simultaneous corrosive and abrasive wear. Journal of Biomedical Materials Research Part B: Applied. 2006; 78B (1): 105–114.
[25] Xu C. Effects of particle size and matrix grain size and volume fraction of particles on the toughening of ceramic composite by thermal residual stress. Ceramics International.2005; 31: 537–542.
[26] Ritasaloa R, Antonov M, Veintha R, and Hannula S. Comparison of the wear and frictional properties of Cu matrix composites prepared by pulsed electric current sintering. Proceedings of the Estonian Academy of Sciences.2014; 63(1): 62-66.